

Gravity Anomaly Matching Technique for Underwater Navigation



Mohsin Nawaz
Regn. # 00000172971

A thesis submitted in partial fulfillment of the requirements
for the degree of **Master of Science**
in
Mathematics

Supervised by: Dr. Matloob Anwar
Co-Supervised by: Dr. Muhammad Ramzan

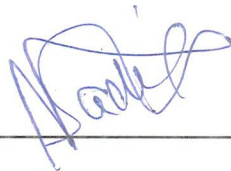
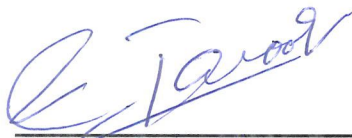

Department of Mathematics

School of Natural Sciences
National University of Sciences and Technology
H-12, Islamabad, Pakistan

2018

National University of Sciences & Technology**MS THESIS WORK**

We hereby recommend that the dissertation prepared under our supervision by: Mohsin Nawaz, Regn No. 00000172971 Titled: Gravity Anomaly Matching Technique For Underwater Navigation accepted in partial fulfillment of the requirements for the award of **MS** degree.

Examination Committee Members1. Name: DR. MUJEEB-UR-REHMANSignature: 2. Name: DR. MUHAMMAD SADIQSignature: External Examiner: DR. BABAR RASHIDSignature: Supervisor's Name DR. MATLOOB ANWARSignature: Co-Supervisor's Name DR. M. RAMZANSignature: 

Head of Department

29/11/2018

Date

COUNTERSIGNEDDate: 29/11/18
Dean/Principal

THESIS ACCEPTANCE CERTIFICATE

Certified that final copy of MS thesis written by Mr. Mohsin Nawaz, (Registration No. 00000172971), of School of Natural Sciences has been vetted by undersigned, found complete in all respects as per NUST statutes/regulations, is free of plagiarism, errors, and mistakes and is accepted as partial fulfillment for award of MS/M.Phil degree. It is further certified that necessary amendments as pointed out by GEC members and external examiner of the scholar have also been incorporated in the said thesis.

Signature: _____ 

Name of Supervisor: Dr. Matloob Anwar

Date: 29/11/2018

Signature (HoD): _____ 

Date: 29/11/2018

Signature (Dean/Principal): _____ 

Date: 29/11/18

Dedicated

to

My Beloved Parents

Acknowledgements

All praise to Almighty Allah and His beloved Prophet Hazarat Muhammad (P.B.U.H.). I would like to express my sincere gratitude to my supervisor, Dr. Matloob Anwer, whose guidance, and continuous encouragement and support right from the start to the end enabled me to successfully complete this work. I would like to express the deepest appreciation to my co-supervisor, Dr. Muhammad Ramzan for helping me in understanding the problem and the relevant concepts. Also I would like to thank Dr. Mujeeb-Ur-Rehman, Dr. Muhammad Sadiq and Mr. Aneeque Ahmed Qazi for their valuable advices and suggestions. I take this opportunity to record my sincere thanks to all the faculty and staff members of SNS for providing valuable guidance always.

There is no words to thank my parents who supported me over the years and always inspired me. I offer gratitude to my brother Hassan Nawaz Butt for being there always and for supporting me through out my life. I would like to recognize Syed Sabyel Haider and Adnan Najum for providing me help during my research work. These acknowledgments would not be complete without mentioning my friends: Muhammad Umair, Muhammad Aleem, Muhammad Asif, Zain-Ul-Abdin, Amir Rahim, Muhammad Huzaifa, Muhammad Ismail, Zeshan Zulifqar and Talmeez-Ur-Rehman. I would like to thank them for their support and encouragement. I am pleased to have such jolly fellows who have always brought smile to my face.

Abstract

Inertial navigation system (INS) is mainly used for navigation purpose in underwater vehicles. However, due to instrumental drifts, INS error accumulates over time and it becomes difficult to ensure the positioning precision during long term missions. Recently, considerable attention has been given to induce corrections as an aid to INS using alternate navigation methods. For this purpose, gravity anomaly aided navigation technique has been explored for underwater applications. The gravity, being an independent passively measured factor, has proven to be a very useful aid for INS corrections. In this technique, appropriate matching area selection is a leading problem, particularly for the application of underwater vehicles. This study focuses on the comparison of suitable area selected by the threshold method and the Principal Component Analysis (PCA) method. In the threshold method selection criteria for matching area was given by using local gravity standard deviation and local gravity correlation coefficient as quantity parameters for selecting matching area while the PCA method is used to integrate local gravity field standard deviation, roughness, slope and correlation coefficients to obtain the final comprehensive characteristic indicator. Finally, we can select the suitable and unsuitable matching regions for navigation by setting a threshold value of the final comprehensive indicator. By using the gravity anomaly reference map of Pakistan area and 0.2 as a threshold value of the final comprehensive indicator, we can select the appropriate area for navigation based on the richness of gravity field information. The results of study validate the use of the proposed technique for real-time applications. PCA is found more appropriate as compared to threshold method for selection of suitable area.

Contents

List of figures	viii
List of Tables	x
1 Introduction	1
1.1 Brief History	1
1.2 Inertial Navigation System (INS)	4
1.3 Auxiliary Inertial Navigation System	5
1.4 Gravity Aided Inertial Navigation System	8
1.5 Gravity Matching Algorithm	9
1.6 Preliminaries	10
1.6.1 Standard Deviation	10
1.6.2 Surface Roughness	10
1.6.3 Correlation Coefficient	10
1.6.4 Normalization	11
2 Gravity Measurement and Gravity Maps	12
2.1 Gravity Measurements	13
2.1.1 Gravity Measuring Devices	13
2.1.2 Satellite Survey Technology	15
2.1.3 Gravity Field Information Calculation	17
2.2 Map Matching Algorithms	18

2.2.1	TERCOM Matching Algorithm	19
2.2.2	ICCP Matching Algorithm	20
2.3	Chapter Summary	21
3	Gravity Field Adaptation Area Selection Criteria	22
3.1	Characteristic Analysis and Matching Area Selection of Gravity Field .	22
3.2	Gravity Field Characteristic Parameters	23
3.2.1	Local Gravity Field Standard Deviation	23
3.2.2	Absolute Roughness of Local Gravity Field	24
3.2.3	Local Gravity Field Slope	26
3.2.4	Correlation Coefficient of Gravity Field	28
3.3	Traditional Adaptation Area Selection Criterion	30
3.3.1	Threshold Method	30
3.3.2	Analytic Hierarchy Process	31
3.3.3	SPSS Regression Analysis	33
3.4	Chapter Summary	34
4	Selection Criteria of Gravity Field Adaptation Area Based on Prin-	
	cipal Component Analysis Method	35
4.1	Principle of Principal Component Analysis (PCA)	35
4.1.1	Fundamentals of PCA	36
4.1.2	Mathematical Model of PCA	36
4.1.3	Steps to Carry Out PCA	37
4.2	Experimental Results	37
4.2.1	Data Analysis and Processing	37
4.2.2	Processing of Gravity Field Characteristic Parameters Based on PCA	39
4.2.3	Implementation Steps of PCA	39

4.3	Experimental Verification	44
4.3.1	Experimental Scheme	44
4.3.2	Results and analysis	44
4.4	Chapter Summary	46
5	Conclusion	47
	Bibliography	48
	Appendix	52

List of Figures

1.1	Schematic diagram of gravity aided inertial navigation system.	8
2.1	Satellite altimetry.	16
2.2	Satellite gravity measurement.	17
2.3	ICCP schematic diagram.	20
3.1	Contour map of standard deviation of gravity field.	24
3.2	Contour map of longitude direction roughness of gravity field.	25
3.3	Contour map of latitude direction roughness of gravity field.	26
3.4	Contour map of longitude slope of gravity field.	27
3.5	Contour map of latitude slope of gravity field.	27
3.6	Contour map of longitude direction correlation coefficient of gravity field.	29
3.7	Contour map of latitude direction correlation coefficient of gravity field.	29
3.8	Binary graph of experimental area by threshold method.	30
3.9	Binary graph of experimental area by AHP.	32
4.1	Gravity anomaly surface map of experimental area.	38
4.2	Gravity anomaly contour map of experimental area.	38
4.3	Richness of gravity field information of experimental area.	43
4.4	Binary graph of experimental area by PCA method.	43
4.5	The matching effect in suitable matching area.	45
4.6	The matching effect in unsuitable matching area.	45

List of Tables

3.1	Normalization criteria.	31
4.1	Correlation Coefficients Matrix.	40
4.2	Principal Component Analysis Extraction of Variance Decomposition.	41
4.3	Component load matrix.	41

Chapter 1

Introduction

1.1 Brief History

As we know, the ocean occupies about 70% of the earth's surface. Today, the land resources are increasingly exhausted. The huge resources of the ocean provide a guarantee for the future development of mankind. In addition, due to the development of modern science and technology, the ocean plays an important role in the national security affairs of coastal countries. Countries have spared no effort to develop various underwater equipment, such as underwater resource detectors, unmanned underwater detectors and submarines for reconnaissance and combat. Because of the particularity of the working environment of the underwater vehicles, it is impossible for the underwater vehicle to navigate and locate by the signals of the satellite navigation system, astronomical navigation system and so on. Inertial navigation system has become the key equipment for underwater vehicle to get the navigation and positioning results.

Inertial navigation system is a relative positioning method based on Newtonian mechanics, which obtains the carrier state by integral operation. The inertial navigation system uses gyroscope and accelerometer as sensitive devices to acquire navigation information. Given the initial state, the system can establish the corresponding attitude matrix according to the output of gyroscope and calculate the output of accelerometer in the corresponding coordinate system according to the established attitude matrix, so as to obtain the three-dimensional positioning and coordinate of the carrier. Because the inertial navigation system works on the basis of inertial principle, it does not

need to transmit signals to the outside world, nor does it need external information. It has the characteristics of independence, autonomy and concealment. Moreover, its navigation performance is stable and reliable in the short term and its data acquisition frequency is high. It has become an important means of autonomous navigation for underwater vehicles [1].

However, the pure inertial navigation system also has its own insurmountable shortcomings, because it uses the tax calculation method to calculate the state information of the carrier, so that the error of the inertial system solution is accumulating which ultimately affects the accuracy and reliability of the navigation solution and even leads to divergence. The observation data of the gyroscope and accelerometer in the inertial navigation system have some errors, such as zero deviation error, zero deviation instability error, random walk error and so on. There is also corresponding error in the installation of inertial instrument. These errors are accumulated by integral calculations. For example, in INS positioning with accuracy better than 1 n mile/h, the zero drift of accelerometer is better than $37\mu g$ and the drift speed of gyroscope is better than $0.0045^\circ/h$. For underwater vehicles with relatively slow motion, the speed is generally between 10 knots to 25 knots and the latent sailing time sometimes reaches 30 days. Even with the inertial navigation system with positioning accuracy of 1 n mile/24h, it accumulates over time. The positioning error is also considerable and it is still difficult to meet the long-range/long-time high-precision navigation positioning requirements [1, 2].

In order to solve the problem of accumulated inertial navigation error, the error of this kind of hardware can be reduced by improving the performance of gyroscope and accelerometer in inertial navigation system. However, the inertial navigation sensor itself is a very precise instrument, its manufacturing process is extremely complex, it is very difficult to continue to further improve the hardware performance of the inertial navigation system. The performance of inertial instruments needs to be improved slightly at a higher cost, while the development of multi-system navigation and positioning mode costs less and has obvious advantages. Therefore, combining other passive autonomous navigation and positioning systems with inertial navigation sys-

tems, making use of the advantages and disadvantages of different navigation systems, learning from each other's strengths and weaknesses, overcoming the shortcomings of accumulating errors in single inertial navigation system is the development trend of underwater vehicle navigation system [1].

The autonomous navigation methods of the front underwater vehicle mainly include acoustic navigation, terrain/landscape matching navigation, geomagnetic field matching navigation and so on. When using acoustics for navigation and positioning, the underwater vehicle needs to reach the location of the acoustic positioning system equipment to receive or transmit relevant signals for positioning and calibration of the inertial navigation sensor. The distance of the underwater vehicle is thus limited and the concealment is also reduced; when terrain / landscape matching navigation, multi-beam, laser or sonar is used. It is easy for underwater carriers to expose their tracks when transmitting signals to measure the depth or topography of the seabed and the terrain/topography matching navigation needs high-precision and high-resolution background data of the seabed topography in the navigation area, which is not easy to obtain. In the geomagnetic field matching navigation, although it does not need to transmit signals to the outside. The application of geomagnetic field matching aided inertial navigation is limited because of the time-varying geomagnetic field, the longer time of updating geomagnetic field model (IGRF, CGRF, etc.), the lower accuracy (error above $100nT$) and the interference of the carrier equipment to magnetic measurement [2, 3].

The earth gravity field is one of the inherent physical characteristics of the earth. It has strong stability and anti-interference. Its distribution is not constant and there is a changing topology. The gravity-related observations of the underwater vehicle can be obtained by the high-precision marine gravimeter and the gravity information of the relevant area can be obtained from the gravity field background map by using the position information given by INS. The gravity information obtained from the actual measurement can be compared with the gravity information extracted from the gravity background map and the positioning error of the inertial navigation system with respect to the state of the carrier can be obtained. Then the error of inertial navigation system

can be corrected. This is the basic principle of gravity field matching aided inertial navigation technology [2].

The US Navy first proposed a theoretical study of gravity-assisted navigation in a military research program conducted in the 1970s to improve the underwater navigation capability of a military submarine. The research of gravity field aided navigation has mainly gone through three stages: before the mid-1980s, the research mainly focused on gravity measuring instruments and gravity navigation theory; since 1990s, the theory of gravity gradient matching navigation has been studied; after 1990s, the matching object has been extended to gravity anomaly, in which on the basis of previous studies, the research on high-precision passive navigation is carried out.

1.2 Inertial Navigation System (INS)

Inertial Navigation System (INS) is a widely used autonomous navigation system, its characteristic is that it can be independently conducted without exchanging information with the outside world, and can work underwater [2, 3, 4]. The basis of inertial navigation is Newton's law, the principle is to measure the acceleration of the carrier in the inertial reference frame. After integrating the time, velocity and deflection angle, the position information can be obtained, so the inertial navigation system can continuously measure the position of the carrier. The function of the gyroscope in the inertial navigation system is to update the navigation coordinate system. The function of the accelerometer is to measure the acceleration of the carrier and the velocity and distance can be obtained by integrating the measured acceleration in the navigation coordinate system.

Gyroscope and accelerometer are the core components of inertial navigation system [5]. Gyroscope and accelerometer zero offset are the key factors affecting the accuracy of inertial navigation system [6, 7], therefore, how to improve the measurement accuracy of gyroscope and accelerometer is the research focus of inertial navigation. The traditional gyroscope mainly refers to the mechanical gyroscope, its structure is complex, and the precision is restricted by many aspects. Since 1970, the modern gyroscope

entered a new period of development. After 80s, Fiber optic gyroscope was developed very rapidly [8, 9]. The advantages of Fiber optic gyroscope are compact structure, reliable work, high sensitivity. At the same time, laser gyroscope [10] and integrated vibratory gyroscope (MEMS gyroscope) have been developed, MEMS gyroscope has higher integration and smaller volume [11]. The initial drift rate of the ball bearing gyroscope is $1\sim 2^\circ/\text{h}$, The precision of the later air-floating, magnetic and liquid-floating gyroscope can reach $0.001^\circ/\text{h}$, while the precision of electrostatic supporting gyroscope is better than $0.0001^\circ/\text{h}$ [12]. Accelerometer is another key component of inertial navigation system, different occasions require different accelerometer performance, the resolution of the accelerometer of the high precision inertial navigation system must reach $0.001g$, but there is no requirement for the range of measurement; However, the accelerometer for measuring the overload of the flying body requires that the range must be $10g$, and there is no requirement for precision [13].

Inertial navigation system has the advantages of good concealment and no interference from outside, but also has the advantages of low noise and good continuity, fast data update and high short-term precision. The navigation task is completed by calculation, and no signal of light electromagnetic is emitted to the outside, so it has good autonomy and concealment, and its work is not limited by time and space, and short-term navigation and positioning are highly reliable. These advantages make inertial navigation technology widely used in aerospace, marine and aerospace fields. It has been widely used in navigation and positioning of various aircraft, missiles, aerospace equipment, tanks, surface ships and underwater carriers. The disadvantages are: the error will increase with time, long-term accuracy is low; initial alignment is required before each use, and the time is longer; the cost is higher and there is no time information.

1.3 Auxiliary Inertial Navigation System

In order to overcome the disadvantage of inertial navigation system (INS), positioning error accumulating over time, the traditional land-based methods usually adopt the

equivalent zero-speed correction and position measurement correction methods. For underwater navigation, in the early 1960s, the position was mostly corrected by astronomical navigation & radio navigation, and the speed was corrected by electromagnetic log [14]. In the 1970s, Roland-C and Meridian were used to correct the position; in the 1980s, underwater acoustic transponders were used to correct the position; after the 1990s, GPS was used to correct the position and acoustic correlation log was used to correct the speed. However, the above method does not meet the requirements of the 21st century for underwater navigation "autonomous, long-time, high-precision, high concealment". The use of astronomical navigation-assisted inertial navigation systems requires underwater carriers to navigate at high altitudes. The use of radio and satellite navigation systems requires underwater submersibles to be exposed to the surface or near the surface of the water to receive information, which is not only time taking and energy consuming, but also has a danger of exposure. In order to overcome the shortcomings of traditional navigation technology and to adapt new technological developments, scholars have carried out research on new integrated navigation methods, mainly focusing on passive navigation technology, with the aim of developing integrated navigation systems that do not rely on GPS.

Underwater passive navigation technology is an important development of modern navigation. In recent years, the geophysical field based navigation has attracted the attention of researchers. This technology uses the characteristics of geophysical fields for navigation and positioning of underwater vehicles. At present, geophysical field navigation technology mainly includes underwater geomagnetic field aided navigation, terrain matching navigation and gravity aided inertial navigation.

The principle of terrain matching navigation is on the basis of acoustic technology, using high speed computer to image the underwater topography and geomorphology, by extracting the feature values and match the three-dimensional map of the pre-existing computer, so as to determine the position, speed and orientation information of the carrier. Terrain matching navigation is not easily interfered by the outside world. It not only has the function of automatic north seeking, but also can accurately calculate the carrier trajectory, speed and azimuth information. However, its disadvantage is

that the terrain matching navigation can be carried out in the pre-explored waters and the depth of the water is limited. The measurement of the seabed contour requires the use of sonar, so the concealment is not high [15, 16, 17].

The geomagnetic field matching navigation needs to draw the characteristic quantity of the geomagnetic field (the magnetic field strength on each of the x, y and z axes and the total magnetic field strength B, etc.) into a reference map, which is stored in a computer when the carrier passes through a certain area, the characteristic quantities of the geomagnetic field passing through this area can be measured in real time by a geomagnetic measuring instrument that is sensitive to the magnetic field and a real-time geomagnetic feature map similar to the topographic feature map is constructed. The map is correlated with the pre-stored reference map and the current state of the vector is calculated. The position is provided to the inertial navigation system (INS) for real-time correction to improve the inertial navigation accuracy. Geomagnetic sensor can automatically find north, small volume, no need to initialize, simple operation, low cost, suitable for small carrier underwater navigation. However, the geomagnetic sensor is easily interfered by the external magnetic field, the accuracy is low, the acceleration cannot be sensed and the high-precision trajectory calculation requirements cannot be satisfied [18, 19].

Gravity aided inertial navigation system uses gravity anomaly or gravity gradient value to correct the error accumulated with time, which has the advantages of concealment, good real-time performance and high precision [2, 20, 21, 22]. The principle of underwater gravity aided inertial navigation system is to store the gravity anomaly data of the navigation area in the navigation computer in advance. By using pre-stored data the characteristic parameters of gravity are calculated to select the suitable area which is used to search the expected path according to the gravity characteristics and to track the route through the kalman filtering technique or the optimization method. In the process, the timing entry is used to match the inertial navigation information and the gravity information with multiple matching algorithms and filter fusion algorithms is used to achieve the purpose of positioning correction, so that the carrier can reach the destination accurately.

1.4 Gravity Aided Inertial Navigation System

Gravity data is an inherent property of the earth that does not change with space and time and its measurement does not require the use of equipment other than gravity instruments. When the carrier is running, the gravity matching is used to correct the error in real time, so that the concealment of the carrier can be ensured. The gravity matching is used to transmit the position information indicated by the inertial navigation system together with the position information in the pre-stored gravity map corresponding to the gravity information measured by the gravity sensor in real time. By using the matching techniques, the matching trajectory is formed closest to the real trajectory and results are fused with the inertial navigation indicator and the inertial navigation error is corrected in real time.

Gravity-aided inertial navigation systems are mainly based on inertial navigation. They are mainly divided into four parts: inertial navigation system, pre-stored gravity reference map (background map), measured gravity parameters (gravimeter, sounding/sweeping instrument, etc.) and matching algorithm.

The schematic diagram is shown in figure 1.1.

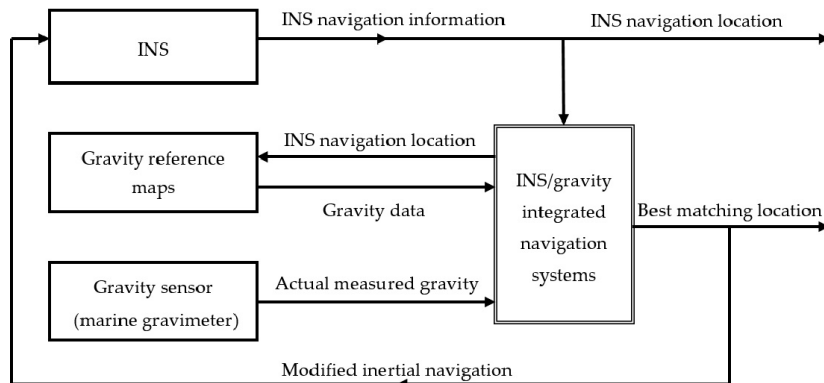


Figure 1.1: Schematic diagram of gravity aided inertial navigation system.

1.5 Gravity Matching Algorithm

The matching algorithm is the core of the gravity aided inertial navigation system. Its precision determines the positioning accuracy and success rate of the integrated navigation system. The matching precision is closely related to the characteristics of the gravity field in the region, the motion characteristics of the underwater vehicle, the detection ability of the gravity sensor and the ocean characteristics (ocean current, monsoon and so on). The matching algorithm requires the ability to detect and process information that contains noise and error, so as to ensure the positioning accuracy [23, 24].

At present, the matching algorithm can be divided into two kinds: one is the algorithm based on the recursive estimation of the optimal filtering principle, which is represented by the Sandia Inertial Terrain Aided Navigation method (SITAN). The other is based on the principle of correlation analysis, the Terrain Contour Matching (TERCOM) algorithm and the Iterative Closest Contour Point (ICCP) algorithm.

Both ICCP and TERCOM algorithms are sequence matching algorithms, which have poor real-time performance and are very sensitive to heading errors. However, it is not necessary to assume that the gravity field data of the search area is linear or Gaussian and there is no need to know the statistical characteristics of the measured values of the gravimeter the SITAN algorithm is a kalman filtering algorithm, which is point matching and has good real-time performance. However, the matching accuracy is affected by the initial error of the inertial navigation system and its noise and the observed noise model in the kalman filtering equation. The anti-interference ability is not as good as the ICCP and TERCOM algorithms. Moreover, the matching algorithms include particle filter algorithms, neural network algorithms and multi-model adaptive estimation [25, 26, 27].

1.6 Preliminaries

1.6.1 Standard Deviation

The standard deviation σ is defined as the square root of the arithmetic mean square of the deviation between the standard value of each unit of the population and its average.

$$\sigma = \sqrt{\frac{1}{N} \sum_i (X_i - \bar{X})^2}, \quad \text{for, } i = 1, 2, \dots, N. \quad (1.1)$$

The standard deviation reflects the degree of dispersion of a data set. The standard deviation is not necessarily the same for the two sets of data with the same average.

1.6.2 Surface Roughness

Irregularities on any surface occurs or created by any machining process known as surface roughness and it is calculated in Ra value,

$$Ra = \frac{1}{n} \sum_{i=1}^n |y_i|. \quad (1.2)$$

1.6.3 Correlation Coefficient

The Pearson correlation coefficient R is used to measure the relationship between two variables X and Y and the range is between $[-1, 1]$,

$$R = \frac{\sum_{i=1}^n (x_i - \bar{x})(y_i - \bar{y})}{\sqrt{\sum_{i=1}^n (x_i - \bar{x})^2 \cdot \sum_{i=1}^n (y_i - \bar{y})^2}}, \quad (1.3)$$

also

$$R = \frac{Cov(X, Y)}{\sqrt{Var[X] Var[Y]}}.$$

Where $Cov(X, Y)$ is the covariance of X and Y, $Var[X]$ is the variance of X and $Var[Y]$ is the variance of Y. The correlation coefficient is a statistical indicator used to reflect the closeness of the correlation between variables.

1.6.4 Normalization

Data standardization (normalization) processing is a basic work of data mining. Different evaluation indicators often have different dimensions and dimension units. Such situations will affect the results of data analysis, in order to eliminate the dimension between indicators. Impact, data standardization needs to be done to resolve the comparability of data metrics. After the original data is processed by data standardization, each indicator is in the same order of magnitude, which is suitable for comprehensive comparative evaluation. Below are two common normalization methods:

Min-Max Normalization

Also called deviation normalization, is a linear transformation of the original data, so that the results fall into the [0,1] interval, the conversion function is as follows:

$$x^* = \frac{x - \min}{\max - \min}, \quad (1.4)$$

where max is the maximum value of the sample data and min is the minimum value of the sample data. One drawback of this approach is that when new data is added, it can cause changes in max and min, which need to be redefined.

Z-Score Standardization Method

It is also called standard deviation standardization. The processed data conform to the standard normal distribution, i.e. the mean value is 0 and the standard deviation is 1. The conversion function is:

$$x^* = \frac{x - \mu}{\sigma}, \quad (1.5)$$

where μ is the mean of all sample data and σ is the standard deviation of all sample data.

Chapter 2

Gravity Measurement and Gravity Maps

Gravity field measurement system mainly uses gravimeter and gravity gradiometer to obtain gravity field information. The gravity field information includes gravity anomaly, vertical deviation and gravity gradient. The reference map used by the gravity field aided inertial navigation can be mainly divided into a gravity gradient reference map and a gravity anomaly reference map. In contrast, gravity gradient is more advantageous in gravity field aided navigation because it contains five independent information and has higher positioning reliability. However, the global gravity gradient data with pupil accuracy has not been published so far and the measured gravity gradient reference data cannot be obtained. At present, the gravity gradient data (gravity gradient forward modeling) is mainly obtained by using the existing terrain gradient and gravity anomaly data with high precision. The acquisition of gravity anomaly data is much easier and high resolution gravity anomaly data can be downloaded from web sites like: **International Gravimetric Bureau (BGI)**, **National Geophysical Data Center (NGDC)**, **National Geospatial Intelligence Agency (NGA)** and other websites [2, 28].

2.1 Gravity Measurements

The apparent gravity of the objects on the surface of the earth is the combined action of real gravity and centrifugal force generated by the rotation of earth. The calculation of centrifugal force is relatively easy and the exact gravitational attraction of the earth to any position around it is complicated. Because the earth's structure is irregular and the mass distribution is not uniform, the gravitational force at any point can not be calculated by a simple and regular model. The model of the earth's gravitational field calculates the real gravitational field of the earth by the spherical harmonic function. The number of terms and the accuracy of the coefficients of the spherical harmonic function reflect the accuracy of the model in simulating the real gravitational field. The establishment of the model of the earth's gravitational field is the process of solving the spherical harmonic coefficients by using the observed gravitational or gravitational data. Therefore, when the order of spherical harmonic function is fixed, the more observed data and the more reasonable the distribution, the more accurate the gravitational field model will be. The acquisition of the reference data of the former ocean gravity field mainly includes: the method of using the traditional measuring instrument for field measurement and the method of satellite measurement to obtain the numerical calculation according to the existing data [1].

2.1.1 Gravity Measuring Devices

- (1) **Submarine gravity survey:** The relevant equipment for gravity measurement is directly placed on the seabed and the information of the gravity field is measured. The measuring device may be a gravimeter or a gravity gradiometer. The measuring equipment can be placed on the seabed for a long time, so corresponding remote control, telemetry, automatic leveling and communication equipment are needed to meet the system's requirement and data transmission.

The advantage of submarine gravity survey is that the instrument can be installed for a long time and can be free from a series of sea level fluctuations. But its shortcomings are also obvious. First, it requires a series of additional equipment

to support the operation of the system, which undoubtedly increases the cost. Moreover, the working environment is the seabed, which makes the installation of the equipment more laborious and the observation process is cumbersome. In addition, its working place is restricted and can only work in areas with relatively shallow water and relatively smooth seabed terrain.

- (2) **Sea surface (shipborne) gravity survey:** Sea surface gravity survey is to place the gravity surveying instrument on the surveying ship. After planning the track, it will directly measure the gravity while sailing on the sea level. Due to the complex ocean surface environment and the influence of sea wind and waves, there will be many external disturbance factors when the surveying ship sails on the water surface. For example: horizontal acceleration, vertical acceleration, periodic horizontal acceleration, periodic vertical acceleration, rotation effect, eotvos effect and so on.

The disturbing factors of gravity measurement on the sea surface mainly include the following aspects:

Horizontal acceleration: Due to the existence of ocean waves and wind, the surveying ship will be affected by various disturbances in the horizontal direction when sailing on the water surface. The influence of these disturbance factors on the horizontal direction of the measuring vessel is finally reflected in the horizontal acceleration observations of the gravity measurement.

Vertical acceleration: Similar to the horizontal acceleration, it is mainly caused by favorable waves and wind forces, which will be reflected in the vertical acceleration measurements.

Rotation effect: The external resistance causes the surveying ship to rotate, resulting in the effect of gravity observation. When the ship changes its heading along the curve, it affects the radial acceleration measured by gravimeter.

Eotvos effect: Since the earth's surface is curved, the motion of the measuring ship relative to the earth would be like a circular motion with the relative motion

center (approximate to the center of the earth), so it would produce a centrifugal force-like effect. The variation of gravity measurements is called the eotvos effect.

When gravity measurement is carried out on the sea surface, the effects of the above four factors cannot be ignored. In order to obtain more accurate gravity field data, it is necessary to eliminate the influence of these factors in the actual survey. For underwater vehicles, the influence of these disturbances is much smaller than that of the ocean surface due to the different working environment, so the measurement accuracy will be improved accordingly [2, 28].

- (3) Marine airborne gravity survey:** Although the technology of marine gravity measurement on ship is mature, the speed of measurement can not meet the real-time requirement of marine gravity field. The use of marine airborne gravity measurement can greatly improve the acquisition speed of marine gravity field data.

Marine airborne gravity measurements and sea surface gravity measurements are much more complicated than interference. For example, in sea surface gravity measurements, the effect of vertical acceleration can be eliminated by averaging the observations. Moreover, the surveying ship is mainly affected by ocean tides, waves and so on. After these effects are eliminated, the motion of the surveying ship can be regarded as stable and the problem of height variation can be ignored. In airborne gravity measurement, it is difficult to distinguish because of the high speed of the carrier, the frequent height changes and the effects of vertical acceleration on the gravity measurement [1].

2.1.2 Satellite Survey Technology

There are usually two ways to obtain gravity information by satellite survey: one is satellite altimetry, the other is satellite gravity survey. The former is to measure the distance from the satellite to the sea level by using the relevant equipment carried on the satellite (such as microwave radar altimeter). If the position of the satellite is known, the altitude of the sea level can be calculated. Of course, the position of

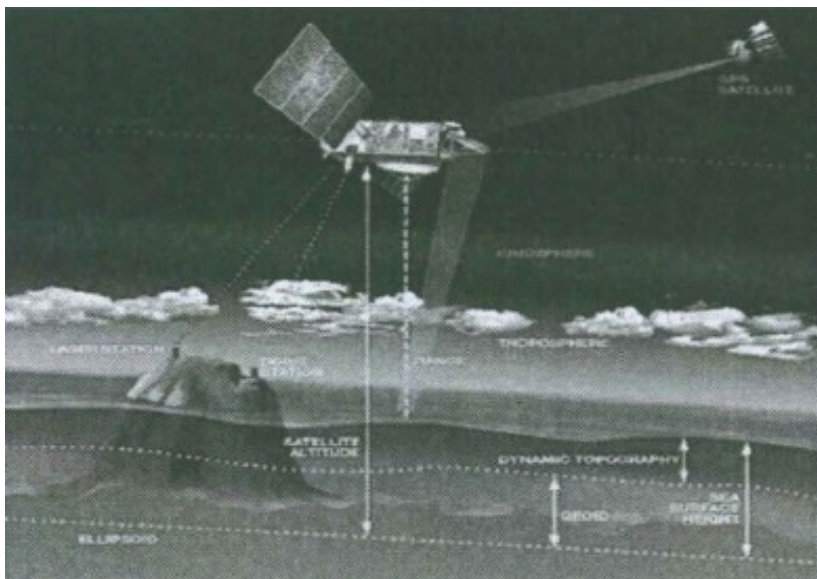


Figure 2.1: Satellite altimetry.

the satellite is also in a certain coordinate system, we can know that if it is in the reference ellipsoid coordinate system, then the calculated sea level height is also in the reference ellipsoid coordinate system, which is equivalent to knowing the height difference between the geoid and the reference ellipsoid, that is, the geoid height. Since the geoid is a gravity equipotential surface, the gravity direction of any point on the surface is perpendicular to it, which is equivalent to obtaining gravity information. However, in this process, satellite orbit determination technology is required to obtain satellite coordinates and in addition to obtaining average sea level temperature, a series of treatments are needed to deduct the interference of various noises such as waves [1]. The latter does not directly measure the sea level, but indirectly deduces the earth's gravity field information from the satellite's orbit around the earth. We can distribute the earth's mass uniformly around a sphere, so that the gravity of a satellite is equivalent to the gravity of a point on the earth's mass at the center of the earth, in this case. The orbit of the next satellite around the earth should be a regular ellipse, which is called the normal orbit. However, the mass distribution of the earth is not uniform and the satellite is also affected by the sun's light pressure and the gravity of the outer celestial bodies, resulting in deviation between the actual orbit

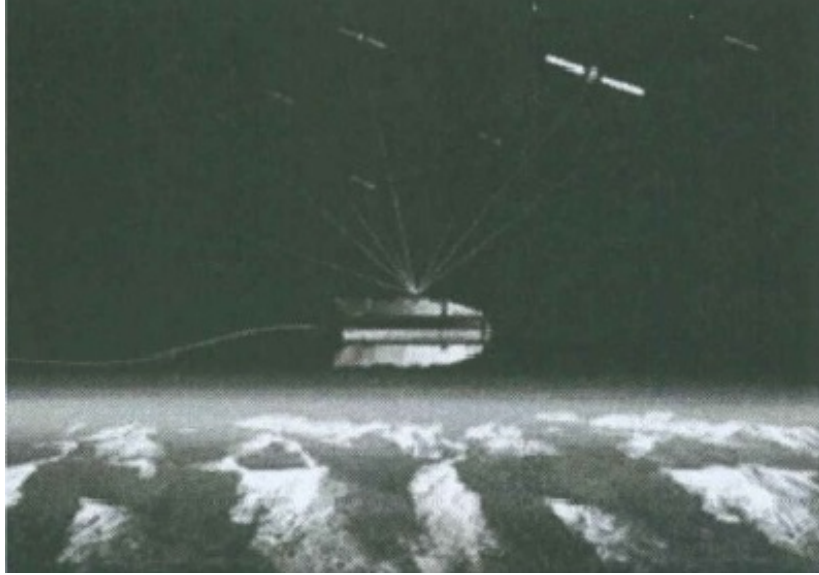


Figure 2.2: Satellite gravity measurement.

and the normal orbit, which is the orbit perturbation. After the orbit perturbation is measured, the influence of solar pressure, atmospheric drag and other perturbation caused by non-earth factors can be deducted. The perturbation part caused by the earth can be obtained and the information of the earth's gravity field can be obtained naturally.

The above two measurement methods have the characteristics of wide measurement area and large amount of data. They have obvious advantages in the acquisition of the vast ocean gravity field data. In recent years, they have made great progress and the accuracy has also developed from the original meter level to the present centimeters level. It can be seen that both of them need the support of satellite orbit determination technology and there are many interference factors to be considered, so there are certain requirements for technology and platform.

2.1.3 Gravity Field Information Calculation

- (1) **Gravity gradient forward modeling:** Gravity gradient is the change of gravity and three-dimensional space. The information of gravity gradient at the same point is more than that of gravity anomaly. Gravity gradient information used in

aided inertial navigation has obvious advantages over gravity anomaly. However, information about gravity gradients is rarely published today, mainly gravity anomaly information.

Gravity gradient measurement has certain advantages. It can directly measure the gradient of the earth's gravity field, so as to avoid the influence of the Eotvos effect. Gravity gradient data acquisition methods include the use of gravity gradiometer observation to simulate the calculation based on the existing gravity field information and terrain, that is, gravity gradient forward modeling.

(2) Inversion of the gravity field model: Since the measured gravity data cannot cover every point on the earth. It can use the existing observation data to build a model of the gravity field that simulates the earth such as the spherical harmonic model mentioned above, in a given point on the earth's surface position can be calculated after the gravity information of the three directions of the point. The pre-existing internationally famous gravity field model is EGM2008, which can obtain a variety of spatial resolution gravity field information, the highest resolution is $1'$ (approximately $1.8km$). Its establishment uses GRACE satellite tracking data, satellite altimetry data and ground gravity data.

(3) Interpolation of ocean gravity field data: The gravity field matching aided navigation needs all the gravity field information of the navigation area as the basis, which can not always be satisfied in practical work. Therefore, it is necessary to use interpolation, fitting and other methods to obtain the existing gravity field information [1, 29].

2.2 Map Matching Algorithms

Map matching is a technique which combines electronic map with location information to obtain the real position of vehicles. A map matching algorithm is used as a key component in improving the performance of navigational systems. This thesis is based

on the terrain contour matching algorithm and iterative closest contour point algorithm given as follows.

2.2.1 TERCOM Matching Algorithm

TERCOM (Terrain Contour Matching) is a correlation extremum matching algorithm, which was first used in terrain aided navigation. The principle is as follows: a set of track points are extracted according to the INS navigation information. Then a series of tracks are selected around the track on the gravity reference map at a certain interval and each sequence is extracted and found in the gravity field reference map. The sequence of gravity measurements is then compared to the actual gravity information and the optimal is considered to be the correct track under certain criteria. The criteria include cross correlation (COR), mean absolute difference (MAD) and mean square difference (MSD) algorithm. According to the existing research, the MSD criterion has the best judgment accuracy and the MAD criterion is the second one. The stability and accuracy of the matching result when COR is used as the judgment principle is worse than the former two algorithms [1, 29, 31, 32].

Generally, the cross correlation algorithm (COR), the mean absolute difference algorithm (MAD) and the mean square difference algorithm (MSD) are defined as:

$$J_{COR} = \frac{1}{n} \sum_{i=1}^n g_r(i)g_m(i), \quad (2.1)$$

$$J_{MAD} = \frac{1}{n} \sum_{i=1}^n |g_r(i) - g_m(i)|, \quad (2.2)$$

$$J_{MSD} = \frac{1}{n} \sum_{i=1}^n [g_r(i) - g_m(i)]^2. \quad (2.3)$$

In the above formula, g_r is the actual gravity anomaly data, g_m is the gravity anomaly map stored data and n is the length of the measured data sequence.

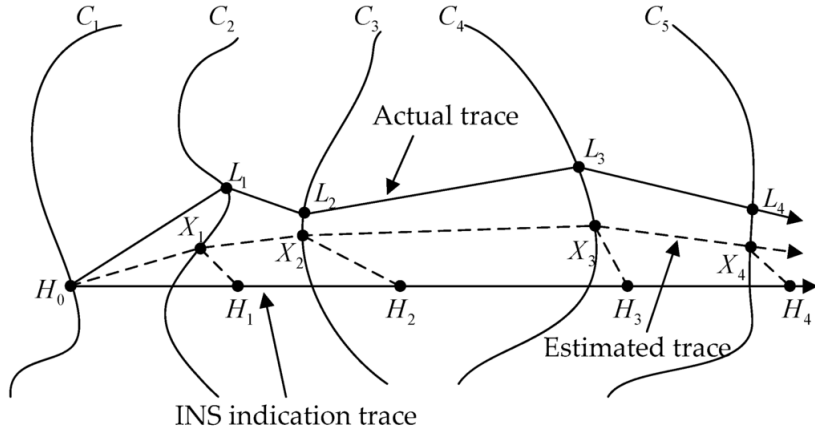


Figure 2.3: ICCP schematic diagram.

2.2.2 ICCP Matching Algorithm

The Iterative Closest Contour Point (ICCP) algorithm was originally used in image processing, but it also used as a matching technique in gravity field matching. It is an image alignment algorithm proposed by Besl et al [28]. The principle of ICCP algorithm is to select a segment of track points sequence on gravity reference map according to INS indication information, then calculate the contour of gravity anomaly observed value corresponding to gravity background map and calculate the adjacent points on the contour line corresponding to each track point to get a group of adjacent points sequence. Since the shapes of the two sequences are not necessarily the same, the center of gravity of the two sequences should be calculated separately. The rotation and translation relations between the two sequences should be calculated, so that the INS indication trajectory can be rigidly transformed to the adjacent point. Repeat the above process. Until the difference between the two adjacent sequences is less than the set threshold, the search can be withdrawn and the last search sequence is taken as the result sequence [2, 28, 33].

In figure 2.3, the sequence H is the INS indicating the trajectory, C is the gravity anomaly contour corresponding to each point P in the sequence H and the sequence L and the sequence X are the iteratively calculated matching sequences. It can be seen intuitively from the graph that the iterative process of matching sequence is actually the

process of correcting the inertial navigation sequence to the optimal sequence [29, 33].

2.3 Chapter Summary

This chapter first introduces several techniques of gravity measurement, including submarine gravity measurement, sea surface gravity measurement, marine airborne gravity measurement, gravity gradient measurement, satellite altimetry technology, gravity field data inversion and data interpolation. Then main matching algorithms linked to gravity aided inertial navigation system are introduced, like TERCOM algorithm and ICCP algorithm. Furthermore, it provides a theoretical basis for improving the matching algorithm.

Chapter 3

Gravity Field Adaptation Area Selection Criteria

The selection of the gravity field adaptation area is the key module of gravity-assisted inertial navigation system. Since the inertial navigation has higher precision in short-time navigation, it is not necessary to always correct the positioning of the inertial navigation. The ideal method is to enter the adaptation zone for correction after a period of voyage, that is, to correct the segmentation. So it is necessary to select a suitable area for the entire navigation area. This chapter introduces the traditional gravity field characteristic parameters and the adaptation region selection methods.

3.1 Characteristic Analysis and Matching Area Selection of Gravity Field

The effect of the local gravitational field on the matching effect should be paid more attention to the relative gravity matching. At the same time, since the change of the gravity field value in the longitude direction is only related to the gravity anomaly at different positions, but in the latitude direction, it is related to the latitude position and its gravity anomaly, so that the gravity field has different characteristics in the longitude direction and the latitude direction. Therefore, the characteristics of the gravity field in both directions of latitude and longitude should be analyzed, which often affect the matching effect of the matching algorithm on the longitude and latitude positions.

The gravity field data is generally stored in a grid matrix. The longitude and latitude span of a gravity field is $M \times N$ grid and $g(i, j)$ is the gravity anomaly value at the grid point coordinates (i, j) . In order to analyze the statistical characteristics of the local gravity field, a local calculation window of size $m \times n$ is defined to calculate the various statistical parameters of the local gravity field. When the center of the calculation window is moved over all the grid points of the entire area, the statistical characteristic values of the respective parts of the entire gravity field area are obtained.

3.2 Gravity Field Characteristic Parameters

The characteristic parameters of the gravity field matching area are important factors affecting the positioning accuracy and matching probability. In the navigation process, gravity matching should be carried out in the region with obvious gravity field characteristics.

The general gravity field characteristic parameters mainly include gravity field's local standard deviation, roughness, slope and correlation coefficient along the longitude and latitude direction. The larger the standard deviation, roughness and slope of gravity field, the smaller the correlation coefficient of latitude and longitude direction. The larger the gravity anomaly change in the adaptation area, which is more favorable for gravity matching.

3.2.1 Local Gravity Field Standard Deviation

Standard deviation is a commonly used statistical distribution measurement parameter [34]. The gravitational field standard deviation σ can measure the dispersion degree of the gravity anomaly sequence. The larger the standard deviation, the richer the gravity field information which can be written as;

$$\sigma = \sqrt{\frac{1}{m(n-1)} \sum_{i=1}^m \sum_{j=1}^n (g(i, j) - \bar{g}_m)^2}, \quad (3.1)$$

where,

$$\bar{g}_m = \frac{1}{mn} \sum_{i=1}^m \sum_{j=1}^n g(i, j). \quad (3.2)$$

A local computation window of size $m \times n$ is selected with the value of m and n

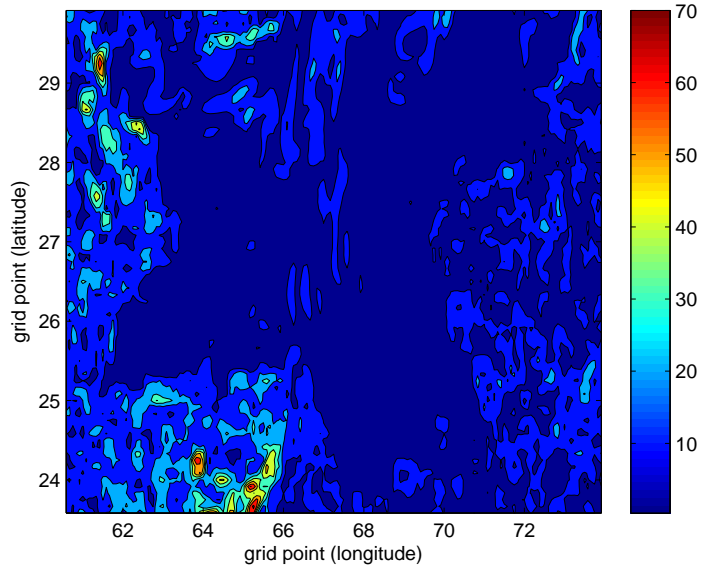


Figure 3.1: Contour map of standard deviation of gravity field.

generally taken as 3 or 5. By using the gravity anomaly reference map of Pakistan area, with resolution $5' \times 5'$, as shown in Fig. 3.1, the gravity anomaly data is obtained through field measurements. The different colors in the figure represent different values. The reddish color area represents the larger standard deviation whereas the blue color represents the smaller standard deviation. The selection criterion for the adaptation area is that the standard deviation should be greater than a certain threshold.

3.2.2 Absolute Roughness of Local Gravity Field

Absolute roughness of local gravity field is a measure of surface smoothness. The greater the roughness means the greater the variation of gravity anomaly [34].

Absolute roughness in longitude direction:

Absolute roughness in longitude direction r_λ is given by the expression;

$$r_\lambda = \frac{1}{(m-1)n} \sum_{i=1}^{m-1} \sum_{j=1}^n |g(i,j) - g(i+1,j)|. \quad (3.3)$$

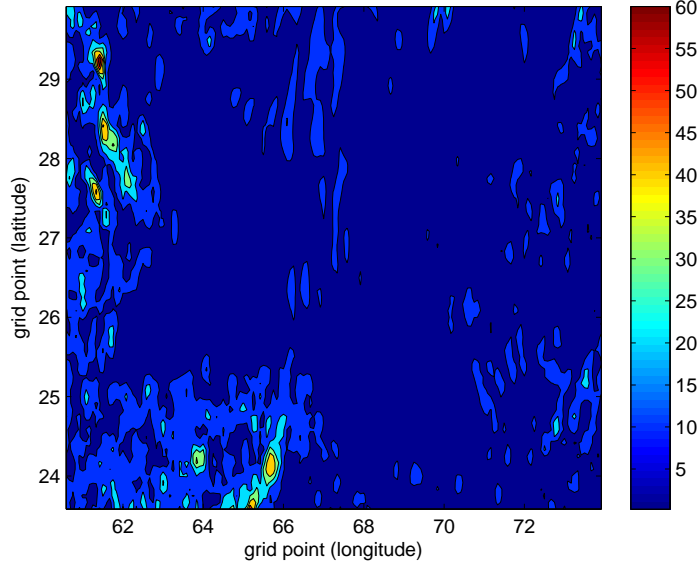


Figure 3.2: Contour map of longitude direction roughness of gravity field.

Absolute roughness in latitude direction:

Absolute roughness in latitude direction r_Φ is given by the expression;

$$r_\Phi = \frac{1}{m(n-1)} \sum_{i=1}^m \sum_{j=1}^{n-1} |g(i,j) - g(i,j+1)|. \quad (3.4)$$

The greater the roughness, the richer the gravitational field features. It can be seen from the Figures 3.3 and 3.2 that the longitude and latitude roughness filling maps are not completely identical. The roughness of the same area is larger in one direction, but is smaller in the other direction. Therefore, the selection criterion of the adaptation area should be that the absolute roughness in the latitude and longitude direction is greater than that of a certain threshold.

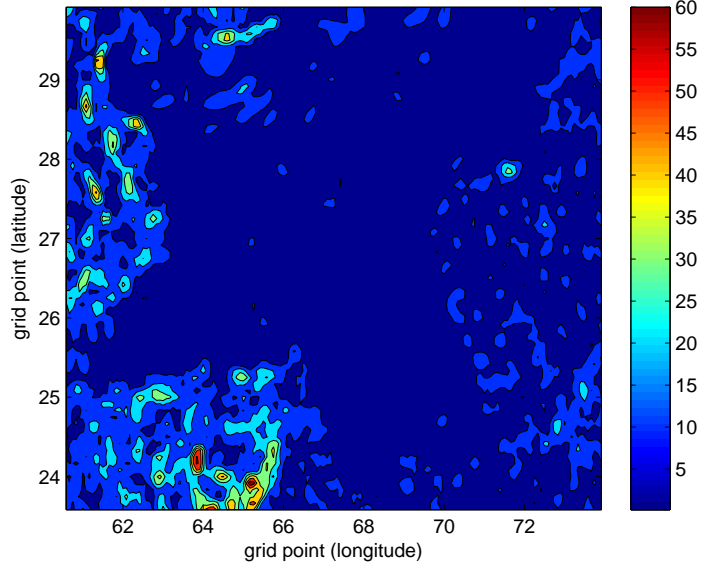


Figure 3.3: Contour map of latitude direction roughness of gravity field.

3.2.3 Local Gravity Field Slope

The slope of gravity field S is the angle between the normal direction and the vertical direction at a certain point on the surface of the gravitational field [34].

Gravity field slope along the longitude:

The slope in longitude direction S_λ is given by the expression;

$$S_\lambda = \frac{1}{6} \left[\begin{array}{c} g(i+1, j+1) + g(i+1, j) + g(i+1, j-1) \\ -g(i-1, j-1) - g(i-1, j) - g(i-1, j+1) \end{array} \right]. \quad (3.5)$$

Gravity field slope along the latitude:

The slope in latitude direction S_λ is given by the expression;

$$S_\Phi = \frac{1}{6} \left[\begin{array}{c} g(i-1, j+1) + g(i, j+1) + g(i+1, j+1) \\ -g(i-1, j-1) - g(i, j-1) - g(i+1, j-1) \end{array} \right]. \quad (3.6)$$

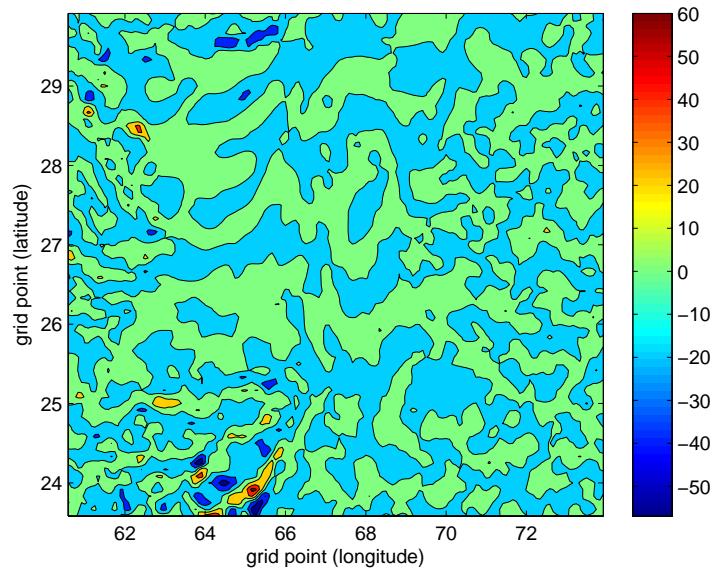


Figure 3.4: Contour map of longitude slope of gravity field.

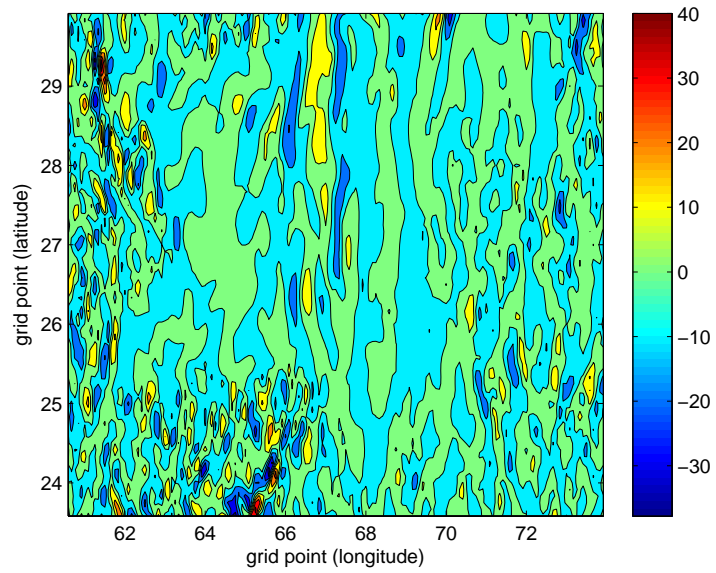


Figure 3.5: Contour map of latitude slope of gravity field.

The expression of slope S is as follows;

$$S = \arctan \left(\sqrt{S_{\lambda}^2 + S_{\Phi}^2} \right). \quad (3.7)$$

Gravity field slope can reflect the degree of change of gravity in both the longitude and latitude direction. When the horizontal distance is the same, the difference between the starting point and the ending point is larger, the slope is larger, the gravity changes faster, and the gravity field slope value is larger, the more suitable for the matching area. So the adaptation area selection criterion is that the gravity field slope is greater than a certain threshold. It can be seen from the Figures that the area with the largest slope of the gravity field is concentrated.

3.2.4 Correlation Coefficient of Gravity Field

The correlation coefficient of gravity field reflects the linear correlation degree of gravity anomaly sequences at adjacent points [34]. For large value of correlation, the adjacent points are highly correlated. Conversely, when adjacent points are less correlated, the gravity anomalies are larger and the positioning is more accurate.

Gravity field longitude direction correlation coefficient

The correlation coefficient R_{λ} along the longitude is expressed as follows;

$$R_{\lambda} = \frac{1}{(m-1)n\sigma^2} \sum_{i=1}^{m-1} \sum_{j=1}^n \left[g(i, j) - \bar{g}_m \right] \left[g(i+1, j) - \bar{g}_m \right]. \quad (3.8)$$

Gravity field latitude direction correlation coefficient

The correlation coefficient R_{Φ} along the latitude is expressed as follows;

$$R_{\Phi} = \frac{1}{m(n-1)\sigma^2} \sum_{i=1}^m \sum_{j=1}^{n-1} \left[g(i, j) - \bar{g}_m \right] \left[g(i, j+1) - \bar{g}_m \right]. \quad (3.9)$$

Figures 3.6 and 3.7 show the correlation coefficient color distribution which is more discrete with smaller local area and the selection criterion of the adaptation area is less than a certain threshold.

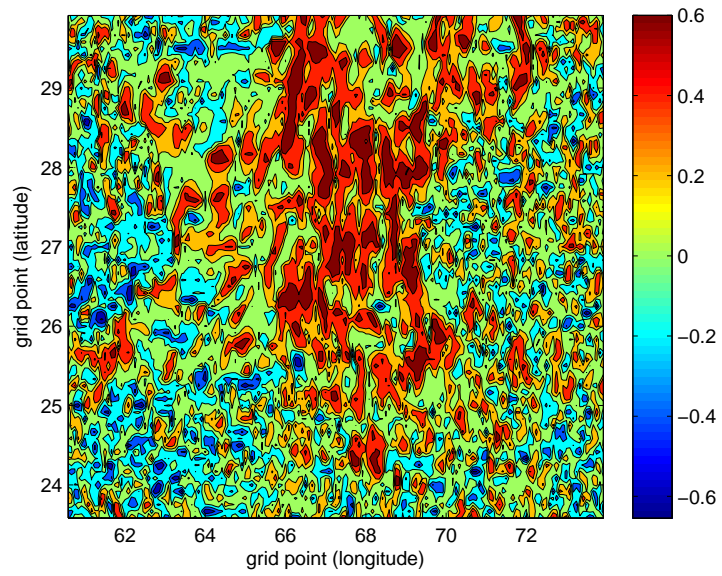


Figure 3.6: Contour map of longitude direction correlation coefficient of gravity field.

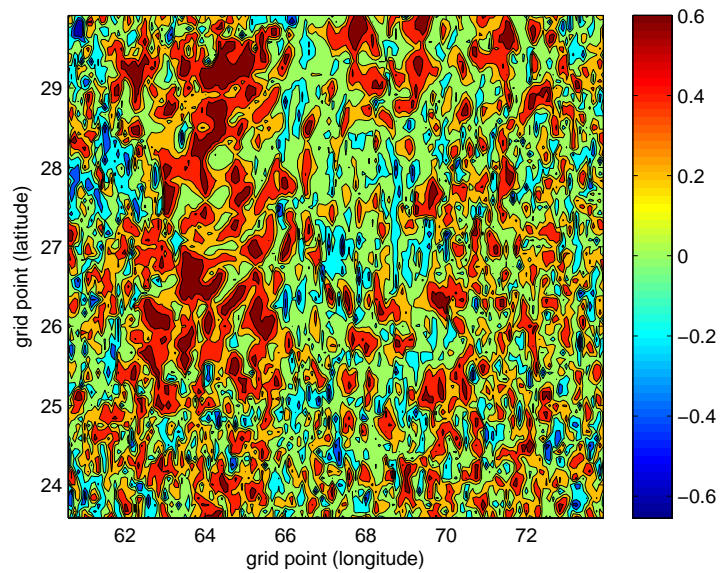


Figure 3.7: Contour map of latitude direction correlation coefficient of gravity field.

3.3 Traditional Adaptation Area Selection Criterion

3.3.1 Threshold Method

The single parameter selection is not accurate for the adaptation area, so the most traditional method is to inter-operate various parameters and select the suitable area. Through the simulation analysis of the second section, we can know that the standard deviation of gravity anomaly can measure the dispersion degree of gravity anomaly of local gravity field. Therefore, in the selection of the adaptation area, a region with a larger standard deviation and a smaller latitude and longitude direction correlation coefficient should be selected [34]. After a large number of simulation experiments, we can use the following matching region experience selection criteria for MSD algorithm and MAD algorithm,

$$\sigma > 4\sigma_s, \wedge R_\lambda < 0.65, \wedge R_\Phi < 0.70, \quad (3.10)$$

where σ_s is the standard deviation of the gravimeter error. In Figure 3.8, the sim-

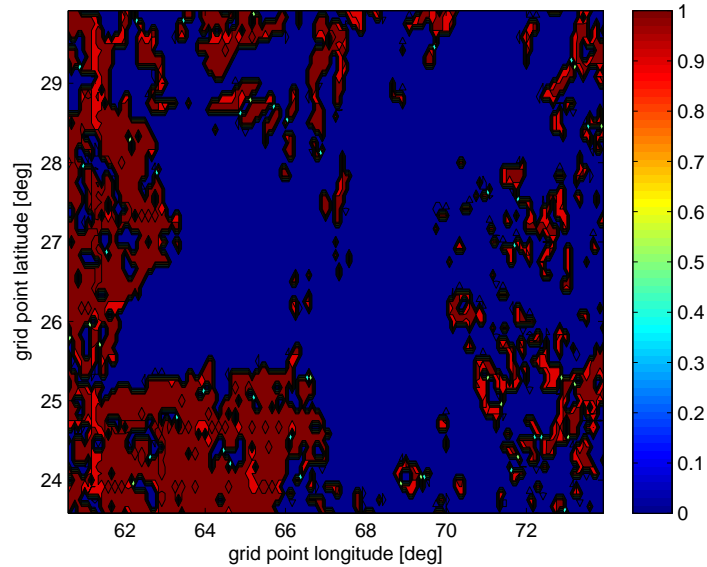


Figure 3.8: Binary graph of experimental area by threshold method.

ulation results of threshold adaptation area are presented. The resolution of gravity

background map is $5' \times 5'$ in the ocean area. The red area in the picture is the selected adaptation area. Most of the adaptation areas in this area are narrow, long and more coherent. It is easy to get out of the adaptation area under the condition of large inertial navigation errors.

3.3.2 Analytic Hierarchy Process

Analytic Hierarchy Process (AHP) is a method that combines multiple feature parameters into a new feature parameter to select the appropriate region. The method requires that the characteristic parameters are normalized, so the feature parameters need to be normalized before the combination and then the analytic hierarchy process is used to measure the gravity anomaly standard deviation, gravity anomaly longitude direction roughness and the gravity anomaly latitude direction roughness. The slope of the gravity anomaly longitude direction and the correlation coefficient of gravity anomaly are combined to obtain the new adaptation region selection criterion, and the adaptation region is selected accordingly [35].

The characteristic parameters are normalized by using the following equation,

$$y = \frac{x - \min(\varphi)}{\max(\varphi) - \min(\varphi)}, \quad (3.11)$$

where y is the normalized characteristic parameter, x is the original feature parameter value, and φ is the data set of the original feature parameter. Based on the characteristics of correlation coefficient, the normalization evaluation criteria of gravity field correlation coefficient is presented in Table 3.1:

Table 3.1 shows the normalized correlation coefficient R of gravity field, if R is 1, it

Table 3.1: Normalization criteria.

Evaluation grade	evaluation criterion	Normalization coefficient
Excellent matching area	$R_\lambda < 0.254 \cap R_\phi < 0.402$	1
Poor matching area	$R_\lambda > 0.254 \cap R_\phi > 0.402$	0
Matching effect is general	Other areas	0.5

indicates that the region with better gravity matching effect, if 0, it is the region with worse gravity matching effect and the other regions with general effect.

Let $C = [c_1, c_2, c_3, c_4, c_5] = [\sigma, r_\lambda, r_\phi, S_\lambda, R]$, which respectively represent the normalized gravity anomaly local standard deviation, gravity anomaly longitudinal roughness, gravity anomaly latitudinal roughness, gravity anomaly longitude direction slope, gravity anomaly correlation coefficient. The characteristics of each feature parameter and its data sensitivity are analyzed. The judgment matrix A can be constructed by the fuzzy rule. The normalized feature vector corresponding to the maximum eigenvalue of matrix A is q and the purpose is to assign weights to each gravity feature parameter. Define a new characteristic parameter $T : T = q^t C$ and select the adaptation area with the characteristic parameter T . The selection criterion is: $T > t_0$, where t_0 is a threshold for dividing the adaptation area and non-adaptation area.

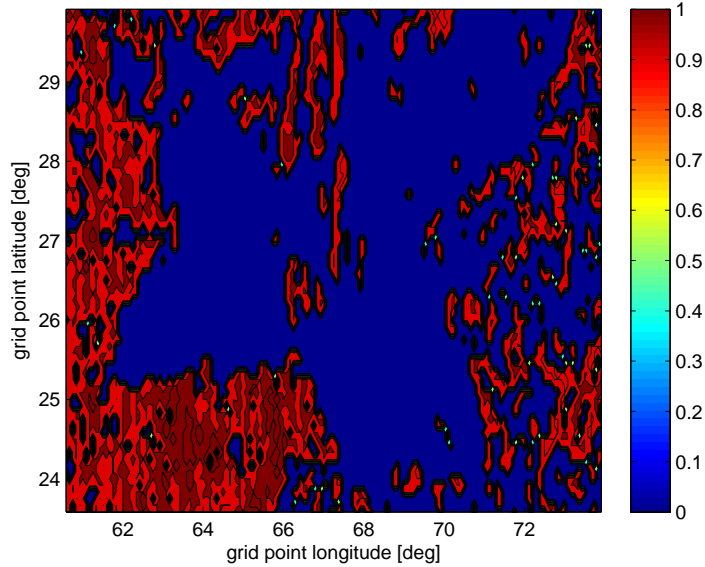


Figure 3.9: Binary graph of experimental area by AHP.

As shown in Figure 3.9, the area selected by the analytic hierarchy process is smaller than that of a single parameter, which is generally in the same area as that of the multiple parameters combined with the threshold method. There is also a situation where the adaptation zone can not be entered when the error is large. Therefore,

although the combination of parameters to select the appropriate region method is better than the threshold selection method of a single parameter, but also has its limitations. The key of this method is to construct the judgment matrix A, and the determination of A depends on the researcher's grasp on the importance of each feature parameter, which is subjectively influenced. Therefore, it is a need of time to study an objective standard adaptation area selection method.

3.3.3 SPSS Regression Analysis

The SPSS regression analysis requires that there must be a region with a known adaptation region. Its principle is to read the gravity anomaly background data, calculate the gravity characteristic parameters of each local region, and select the appropriate gravity features to establish a dimensional formula according to the constraints.

The key to SPSS regression analysis is the accuracy of the pre-stored adaptation zone. First of all the dimensional equation should be established. The basic dimension harmony and π Theorem should be used to establish the dimensional equation. The index of the dimensional equation can be determined by SPSS regression analysis of the gravity characteristic parameters in the pre-stored adaptive region. So that the exact formula of selecting the adaptive region can be established [36].

The SPSS analysis algorithm is mainly dependent on the accuracy of the data in the pre-stored adaptation area. If the pre-stored data is not accurate, the selection error of the adaptation area will be large or even divergent. In the SPSS analysis method, the standard deviation of gravity σ , the gravity gradient α and the correlation coefficient r are generally constructed. The dimensional analysis is based on the π theorem,

$$T = K \cdot \sigma^x \cdot \alpha^y \cdot r_\varphi^m \cdot r_\lambda^n, \quad (3.12)$$

where x, y, m, n are dimension indices. T and K are dimensionless quantities.

The experimental area is $23.5^\circ \sim 30^\circ$ north latitude and $60.5^\circ \sim 74^\circ$ east longitude. Initially, an adaptation area needs to be selected by some other method. The adaptation area needs to be repeatedly verified before it can be used in SPSS. The

area corresponding to the falling edge of the latitude and longitude error in the navigation system must be found first. After being verified as the adaptation area, the SPSS regression analysis algorithm is used for analysis. Through the regression analysis algorithm of SPSS, the obtained relation is as follows;

$$30.853 = \sigma + 37.310r_{\varphi} + 9.784r_{\lambda} - 0.919\alpha. \quad (3.13)$$

The above formula is an accurate measure adaptation zone. Because of the calculation error, it can not be expressed by an equal sign. Therefore, the selection criterion for the suitable region is that the error is not more than 0.01, that is, $30.853 - \sigma + 37.310r_{\varphi} + 9.784r_{\lambda} - 0.919\alpha < 0.01$.

During the experiment, the characteristic parameters of the region are calculated first, and the value is calculated according to the formula on the right side. If the value is within the error range of 30.853, it is considered as the adaptive region; otherwise, it is regarded as the non-adaptive region.

The simulation conditions remain unchanged. It can be seen from the binary graph that the selected adaptive region is not as accurate as a single parameter after the combination of the characteristic parameters by SPSS in the experimental region. The reason is that the SPSS regression analysis method needs a known adaptive region as a reference. Therefore, if the selection of the prior adaptive region is not accurate, the whole adaptation area will be affected. Hence, the selection of a priori adaptation region in SPSS regression analysis is particularly important.

3.4 Chapter Summary

This chapter first introduces several traditional gravity field characteristic parameters to measure the richness of gravity field information, including gravity field local standard deviation, gravity field absolute roughness, gravity field slope and gravity field correlation coefficient. Then by analyzing the traditional gravity field characteristic parameters, the traditional method for selection of the suitable region is simulated and verified.

Chapter 4

Selection Criteria of Gravity Field Adaptation Area Based on Principal Component Analysis Method

The choice of gravity field adaptation area is a crucial step in Gravity-Aided Inertial Navigation System (GAINS), but there are many kinds of characteristic parameters about gravity field. Different characteristic parameters reflect different aspects of gravity field information. How to make full use of different characteristic parameters of gravity field to ensure the loss of original information in an acceptable range has become a key problem in the selection of suitable matching area [34, 35, 36, 37]. In this chapter, Principal Component Analysis (PCA) method is used to synthesize the gravitational field standard deviation, roughness, slope and correlation coefficient into a single weighing indicator for measuring the adaptability of the gravitational field, which provides a certain reference for the selection of the suitable matching area.

4.1 Principle of Principal Component Analysis (PCA)

Principal Component Analysis (PCA) is a simple, nonparametric method for extracting relevant information from complex data sets. It is often used to reduce the dimension of a series of complex and correlated data to obtain a set of independent comprehensive indicators, which some extent can reveal the hidden information in the data [38].

4.1.1 Fundamentals of PCA

Principal Component Analysis (PCA) is probably the oldest and best known technique of multivariate analysis. It was first introduced by Pearson(1901) and developed independently by Hotelling (1933). Like many multivariate methods, it was not widely used until the advent of electronic computers, but it is now well established in virtually every statistical computer package. Principal Component Analysis (PCA) is a simple, non-parametric multivariate technique that analyzes a data sets in which observations are described by several inter-correlated quantitative dependent variables. Its goal is to extract the important information from confusing data sets, to represent it as a set of new orthogonal variables called principal components. It is often used to reduce the dimensionality of a complex and correlational data set. Principal components are uncorrelated and are ordered so that the first few retain most of the variation present in all the original variables. PCA also represents the pattern of similarity of the observations and the variables by displaying them as points in the map [30].

4.1.2 Mathematical Model of PCA

The PCA method can account for most of the variant of the original n indicators via p uncorrelated principal components, where $p \leq n$. Suppose $U = \{U_1, U_2, \dots, U_n\}$ be a set of original indicators with covariance matrix S . By using PCA, a set of uncorrelated indicators which is the linear combination of the original indicators can be obtained as follows [39];

$$\begin{bmatrix} V_1 \\ V_2 \\ \cdot \\ \cdot \\ V_p \end{bmatrix} = \begin{bmatrix} a_{11} & a_{12} & \dots & a_{1p} \\ a_{21} & a_{22} & \dots & a_{2p} \\ \cdot & \cdot & & \cdot \\ \cdot & \cdot & & \cdot \\ a_{n1} & a_{n2} & \dots & a_{np} \end{bmatrix}^T \begin{bmatrix} ZU_1 \\ ZU_2 \\ \cdot \\ \cdot \\ ZU_n \end{bmatrix}, \quad (4.1)$$

$$V = A^T ZU, \quad (4.2)$$

where $V = \{V_1, V_2, \dots, V_p\}^T$ is a set of comprehensive indicators, V_1 is called the first principal component, V_2 is called the second principal component and so on;

$A = a_{ij}(i = 1...p, j = 1...n)$ are the eigenvectors corresponding to the eigenvalues of covariance matrix S of V . $ZU = \{ZU_1, ZU_2, \dots, ZU_n\}$ are the normalized values of $U = \{U_1, U_2, \dots, U_n\}$ [40].

4.1.3 Steps to Carry Out PCA

- (1) The original indicator is selected as per requirement of the problem.
- (2) The original indicator is normalized and its covariance/correlation matrix is calculated.
- (3) The eigenvalues of the covariance/correlation matrix and its corresponding eigenvectors are calculated.
- (4) The expression of principal components is determined based on eigenvalues and eigenvectors.
- (5) Finally to calculate the last comprehensive index and its use to study the problem.

4.2 Experimental Results

In order to check the validity of the PCA method, the experiments with pre-stored gravity map are conducted. The value of characteristic parameters on every gridding point in gravity reference map is obtained.

4.2.1 Data Analysis and Processing

Presently, there is no published global gravity gradient map. Therefore, the gravity anomaly map is selected as the background map in this study. The gravity anomaly reference map of Pakistan area ($60.5^\circ \sim 74^\circ$ longitude and $23.5^\circ \sim 30^\circ$ latitude) with longitude direction interval $5'$, and latitude direction interval is close to $5'$ is used in this work. The unit of gravity anomaly is mGal.

The gravity anomaly surface of experimental area is shown in Figure 4.1 and the gravity anomaly contour plot of experimental area is shown in Figure 4.2.

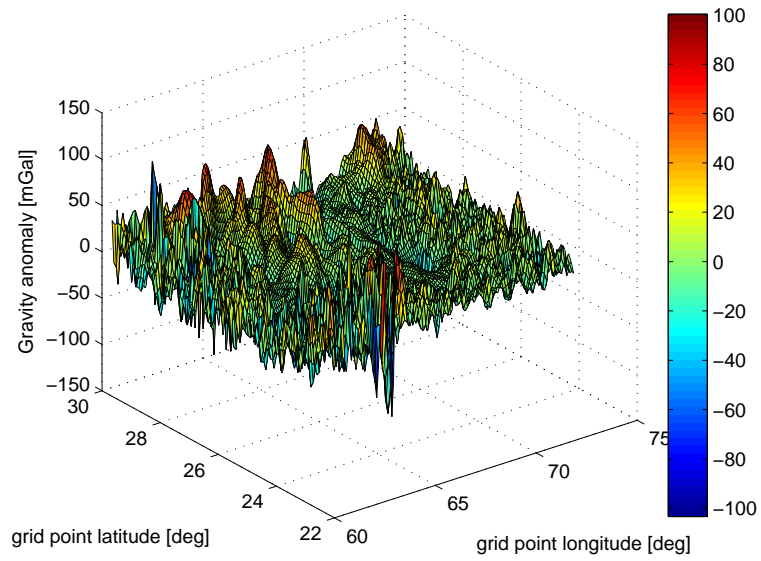


Figure 4.1: Gravity anomaly surface map of experimental area.

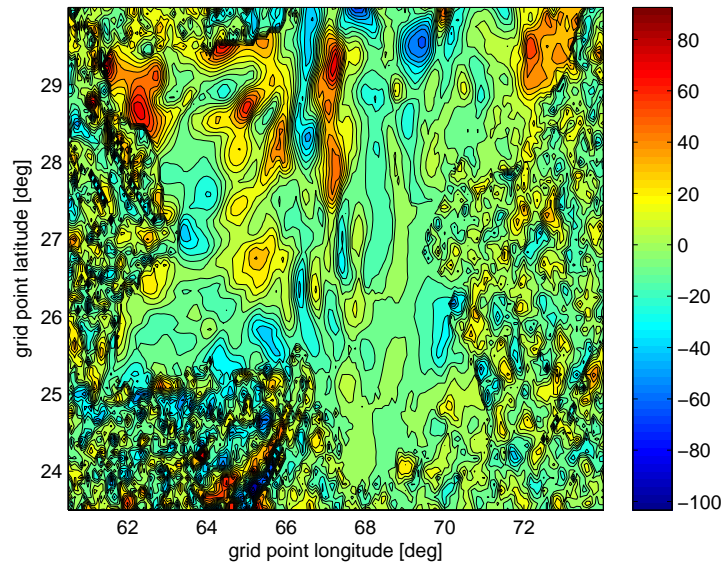


Figure 4.2: Gravity anomaly contour map of experimental area.

4.2.2 Processing of Gravity Field Characteristic Parameters Based on PCA

In this chapter, the standard deviation, roughness, slope and correlation coefficient of gravity field are used as input information of PCA. These parameters have been calculated before PCA processing. The third chapter provides the relevant calculation formulas for the calculation of the characteristic parameters which is not the focus of this research, so the results of PCA are directly presented in this thesis.

4.2.3 Implementation Steps of PCA

Step 1: The original indicator is selected according to the needs of the research problem. In this work, we choose gravity anomaly standard deviation σ , absolute roughness in longitude direction r_λ , absolute roughness in latitude direction r_Φ , slope of gravity anomaly in longitude direction S_λ , slope of gravity anomaly in latitude direction S_Φ , the longitude direction correlation coefficient R_λ and the latitude direction correlation coefficient R_Φ as the original indicators,

$$U = \{\sigma, r_\Phi, r_\lambda, S_\Phi, S_\lambda, R_\Phi, R_\lambda\}. \quad (4.3)$$

Step 2: Principal components are dependent on the units used to measure the the original indicators, we should always normalize the original indicators prior to using PCA method. Two commonly used normalization methods as discussed in Chapter 1 are given by;

First: min-max normalization is to transform all the original indicators in the range [0,1] as follows,

$$ZU_i = \frac{U_i - \min(U_i)}{\max(U_i) - \min(U_i)}, \quad i = 1, \dots, n. \quad (4.4)$$

Second: Z-score standardization method process the original indicators to have zero mean and unit standard deviation as follows,

$$ZU_i = \frac{U_i - \text{Mean}(U_i)}{\text{Standard Deviation}(U_i)}, \quad i = 1, \dots, n. \quad (4.5)$$

After normalization of data find covariance/correlation matrix by using the following formula;

$$S = \frac{1}{m-1}AA^T, \quad (4.6)$$

where A is the matrix of normalized indicators. The Table 4.1 shows the cor-

Table 4.1: Correlation Coefficients Matrix.

Original Indicator	σ	S_Φ	S_λ	r_Φ	r_λ	R_Φ	R_λ
σ	1.000	.042	-.001	.845	.909	.065	-.172
S_Φ	.042	1.000	-.081	.048	.038	.007	-.017
S_λ	-.001	-.081	1.000	-.006	.003	-.004	.004
r_Φ	.845	.048	-.006	1.000	.683	-.327	.027
r_λ	.909	.038	.003	.683	1.000	.208	-.469
R_Φ	.065	.007	-.004	-.327	.208	1.000	-.450
R_λ	-.172	-.017	.004	.027	-.469	-.450	1.000

relation between the seven selected characteristic parameters. The larger the correlation coefficients, the stronger the correlation between the corresponding indicators.

Step 3: Calculate the eigenvalues of the covariance/correlation matrix and its corresponding eigenvectors. The eigenvalues λ_i ($i = 1, \dots, p$) of S are solutions to the characteristic equation,

$$|S - \lambda I| = 0. \quad (4.7)$$

The eigenvalues $\lambda_1, \lambda_2, \dots, \lambda_p$ are the variances of the coordinates on each principal component axis. By sorting the eigenvalues in descending order, the eigenvector with highest eigenvalues is selected as principal component of the data set.

The Table 4.2 shows three eigenvalues greater than 1, indicating that the seven original indicators can be reduced to three principal components.

Table 4.2: Principal Component Analysis Extraction of Variance Decomposition.

Component	Initial Eigenvalues			Extraction Sums of Squared		
	Total	% of Variance	Cumulative %	Total	% of Variance	Cumulative %
1	2.714	38.766	38.766	2.714	38.766	38.766
2	1.606	22.946	61.712	1.606	22.946	61.712
3	1.080	15.422	77.134	1.080	15.422	77.134
4	.917	13.104	90.238			
5	.538	7.691	97.930			
6	.119	1.699	99.628			
7	.026	.372	100.000			

Table 4.3: Component load matrix.

Original Indicators	Components		
	1	2	3
σ	0.966	.119	.023
S_Φ	.073	.005	-.726
S_λ	-.007	.004	.742
r_Φ	.838	.483	.007
r_λ	.962	-.164	.029
R_Φ	.092	-.868	-.003
R_λ	-.372	.760	-.005

Step 4: The expression of principal components is determined based on eigenvalues and eigenvectors. The coefficients to transform the seven original indicators into three principal components can be obtained by dividing the three data sets shown in Table 4.3 by the square root of its corresponding eigenvalues, i.e. $\sqrt{\lambda_i}$, $i = 1, 2, 3$ and the transformation formulas are shown as follow;

$$\begin{aligned}
 V_1 = & 0.5864ZU_1 + 0.0443ZU_2 - 0.0042ZU_3 + 0.5087ZU_4 \\
 & + 0.5839ZU_5 + 0.0558ZU_6 - 0.2258ZU_7,
 \end{aligned} \tag{4.8}$$

$$\begin{aligned}
V_2 = & 0.0939ZU_1 + 0.0039ZU_2 + 0.0032ZU_3 + 0.3811ZU_4 \\
& - 0.1294ZU_5 - 0.6849ZU_6 + 0.5997ZU_7,
\end{aligned} \tag{4.9}$$

$$\begin{aligned}
V_3 = & 0.0221ZU_1 - 0.6986ZU_2 + 0.7140ZU_3 + 0.0067ZU_4 \\
& + 0.0279ZU_5 - 0.0029ZU_6 - 0.0048ZU_7.
\end{aligned} \tag{4.10}$$

Step 5: The three principal components can be further simplified into one final comprehensive index based on the percentages that their corresponding eigenvalues accounted for the sum of three eigenvalues. By multiply the coefficients of each corresponding components by $\lambda_i / \sum_{j=1}^3 \lambda_j$ and by adding the results together we can transform the seven original indicators into one comprehensive indicator, and the transformation formula is given by;

$$F = \sum_{i=1}^3 \frac{\lambda_i}{\sum_{j=1}^3 \lambda_j} V_i, \tag{4.11}$$

where $V_i (i = 1, 2, 3)$ are the three principal components. According to Eq. (4.11), an integrated expression of principal components can be calculated as given in Eq. (4.12).

$$\begin{aligned}
F = & 0.3271ZU_1 - 0.1163ZU_2 + 0.1416ZU_3 + 0.3704ZU_4 \\
& + 0.2606ZU_5 - 0.1762ZU_6 + 0.0639ZU_7.
\end{aligned} \tag{4.12}$$

F is the final comprehensive index to measure the richness information of gravity field. Figure 4.3, shows the gravity field richness information of experimental area. The larger value of the final comprehensive indicator means more abundant gravitational field information. The maximum value of the final comprehensive index of the experimental area is 7.4337 while the minimum value is -1.4858, and the mean value is $5.4183e^{-15}$ which is almost equal to zero. To properly improve the criteria for matching regions, we choose a threshold value slightly larger than the average value of the final composite index, which is 0.2. Figure 4.4, shows the decision results of suitable matching areas and unsuitable matching areas based on final comprehensive index . The red area is suitable while the blue part represents the unsuitable matching area.

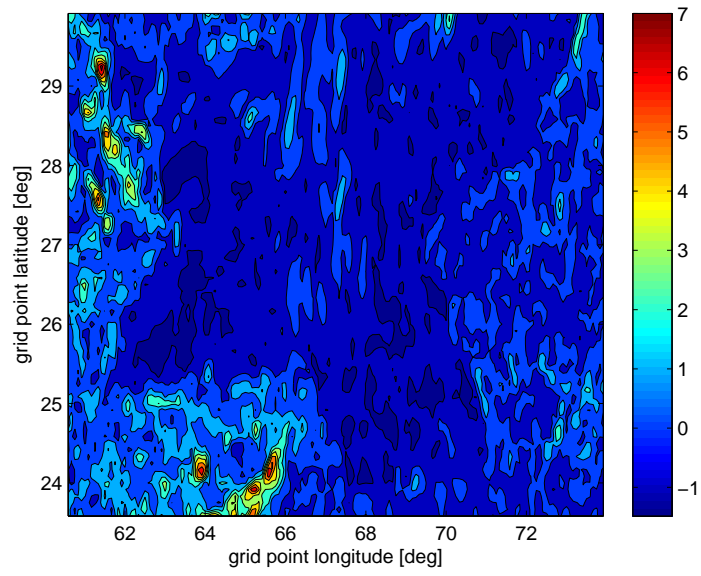


Figure 4.3: Richness of gravity field information of experimental area.

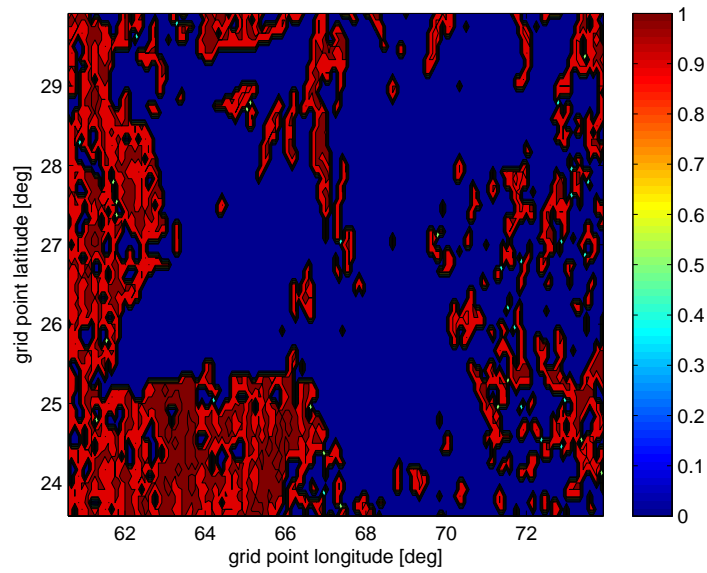


Figure 4.4: Binary graph of experimental area by PCA method.

4.3 Experimental Verification

In order to ensure the effectiveness of the proposed method, the experiments with practical INS data are conducted in the directions which have minimum and maximum matchable points. The parameters of the INS are as follows: the gyroscope drifts of INS in three directions are $0.02^\circ/h$; and the random drifts are $0.01^\circ/h$; the accelerometer bias in three directions are $1 \times 10^{-4}g$, and the random drifts are $5 \times 10^{-4}g$.

4.3.1 Experimental Scheme

Two trajectories were selected in the adaptive region and the non-adaptive region respectively. Each simulation trajectory contains twenty trajectory way points with a sampling interval of $5'$. The carrier travels along the northeast or northwest direction with velocities of 12 n mile/h in longitude and 10 n mile/h in latitude, respectively. In two directions, the random error of INS in the specified location is 0.12 n mile. The error of gravity anomaly measurement is 3 mGal, including measurement and mapping errors. The TERCOM matching algorithm introduced in section 2.3 is verified in the experimental area.

4.3.2 Results and analysis

Figures 4.5 and 4.6 show the matching effect between the adaptation zone and the non adaptation zone. The comparison of two figures roughly shows that the matching effects of the trajectories in suitable matching areas is batter than that in unsuitable matching area as the former gets smaller position deviation.

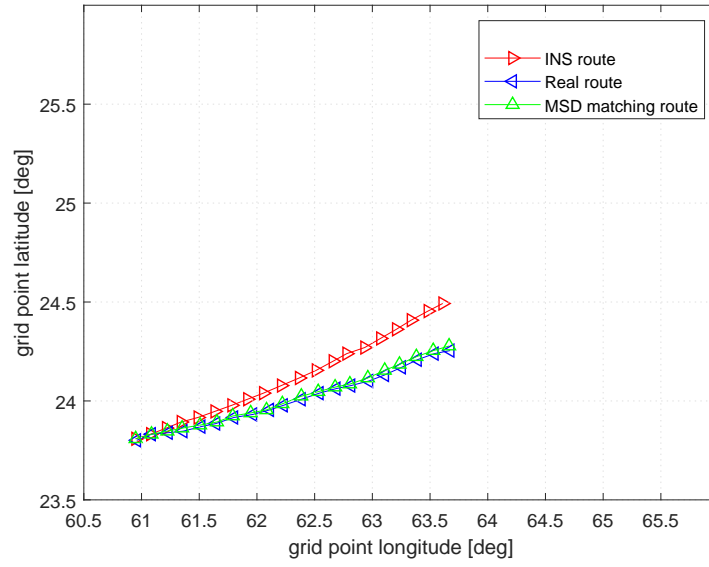


Figure 4.5: The matching effect in suitable matching area.

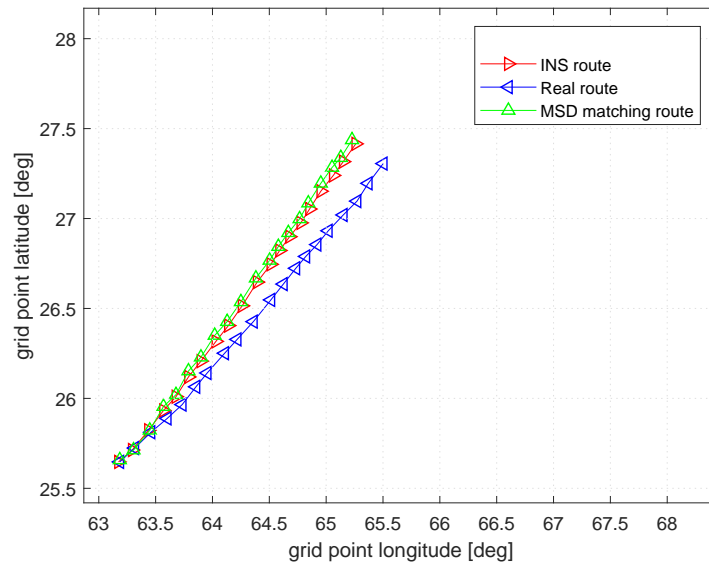


Figure 4.6: The matching effect in unsuitable matching area.

4.4 Chapter Summary

In this chapter, the basic principle of principal component analysis (PCA) method is introduced. Then a method is proposed to determine the suitable matching region by using PCA. The standard deviation, roughness, slope and correlation coefficient of gravity field are integrated into a single index to measure the suitability of gravity field. Then the gravity reference map is divided into adaptive region and non-adaptive region by setting threshold value for the final comprehensive index. Finally, Terrain Contour Matching (TERCOM) algorithm with Mean Square Deviation (MSD) criterion is used to carry out experiments and verify the applicability and reliability of the proposed method.

Chapter 5

Conclusion

The matching performance of gravity matching algorithm based on correlation analysis is closely related to the characteristics of gravity field in the matching region. The number of statistical parameters of local gravity field are calculated by means of a moving local computation window. Comparison between threshold method and principal component analysis (PCA) method for selection of suitable matching region is proposed in this research. In the threshold method, local gravity field standard deviation and the correlation coefficient in the direction of longitude and latitude are finally determined as the criteria for selecting the matching area. Whereas, in the PCA method local gravity field standard deviation, roughness, slope and correlation coefficients are selected as characteristic parameters for the input of PCA, the final comprehensive weighing indicator was obtained to evaluate the matching area selection criteria. Simulation and experimental results ensure that the matching area adopted by PCA method cover all the regions which have larger gravity anomaly variation. The PCA method can select matching region by using only one threshold as compared to three threshold parameters of the threshold method and is found more accurate. Hence, the matching area selected by the PCA method is more valid than threshold method.

Bibliography

- [1] DONG C. Study on Matching Algorithm and Selection of Suitable Matching Area for Underwater Gravity-aided Inertial Navigation System; 2017.
- [2] Li S Shan. Research on Theory and Method of Underwater Gravity Assisted Inertial Navigation; 2010.
- [3] Wang H. Compensation method of gravity disturbance for high precision long endurance inertial navigation system; 2015.
- [4] Chen X, Runtao W. Strapdown inertial navigation algorithm research. Science and Technology Innovation Guide. 2015;**17**:19–22.
- [5] Ren Q, Wang B, Deng Z, Fu M. A multi-position self-calibration method for dual-axis rotational inertial navigation system. Sensors and Actuators A: Physical. 2014;**219**:24–31.
- [6] Wang B, Ren Q, Deng ZH, Fu M. A self-calibration method for nonorthogonal Aangles between gimbals of rotational inertial navigation system. IEEE Trans Industrial Electronics. 2015;**62**:2353–2362.
- [7] Wang B, Deng Z, Liu C, Xia Y, Fu M. Estimation of information sharing error by dynamic deformation between inertial navigation systems. IEEE Transactions on Industrial Electronics. 2014;**1**:2015–2023.
- [8] Wang C. Modeling, analysis and compensation of random drift of fiber optic gyroscope; 2015.

- [9] Liu Z. Research on signal processing and temperature compensation of fiber optic gyroscope; 2015.
- [10] Wang C. Research on Integrated Navigation and Zero Velocity Correction Technology of Laser Gyro Strapdown Inertial Navigation System; 2009.
- [11] Ma C, LANG, Tan Y, Yubin L, Wang S. Design and test of two-axis attitude adjustment system based on MEMS sensor. 2015;**S1**:28–37.
- [12] Zhang J, Zhao J. Research status and development trend of gyroscopes in inertial navigation. 2008;**07**:60–61.
- [13] Gu Y. Overview of Inertial Accelerometer Technology. Aircraft Missile. 2001;**6**:78–84.
- [14] Zhu X, Chai J. Research on the correction of inertial navigation technology using land-based radio ranging information. Modern Electronic Technology. 2009;**32**:152–154.
- [15] Zhao L, Gao N, Huang B, Wang Q, Zhou J. A novel terrain-aided navigation algorithm combined with the TERCOM algorithm and particle filter. IEEE Sensors Journal. 2015;**15**(2):1124–1131.
- [16] Zhu M, Liang D, Yan P. A point pattern matching algorithm based on QR decomposition. Optik-International Journal for Light and Electron Optics. 2014;**125**(14):3485–3490.
- [17] Reynaud S, Louis C. A universal navigability map building approach for improving Terrain-Aided-Navigation accuracy. In: Position Location and Navigation Symposium (PLANS), 2010 IEEE/ION. IEEE; 2010. p. 888–896.
- [18] Liu Y, Wu M, Hu X, Xie H. Research on geomagnetic matching method. In: Industrial Electronics and Applications, 2007. ICIEA 2007. 2nd IEEE Conference on. IEEE; 2007. p. 2707–2711.

- [19] Ma X, Liu H, Xiao D, Li H. Key technologies of geomagnetic aided inertial navigation system. In: Intelligent Vehicles Symposium, 2009 IEEE. IEEE; 2009. p. 464–469.
- [20] Abe M, Kroner C, Förste C, Petrovic S, Barthelmes F, Weise A, et al. A comparison of GRACE-derived temporal gravity variations with observations of six European superconducting gravimeters. *Geophysical Journal International*. 2012;**191**(2):545–556.
- [21] Hirt C, Kuhn M, Claessens S, Pail R, Seitz K, Gruber T. Study of the Earth's short-scale gravity field using the ERTM2160 gravity model. *Computers & Geosciences*. 2014;**73**:71–80.
- [22] Meyer U, Jäggi A, Beutler G. Monthly gravity field solutions based on GRACE observations generated with the Celestial Mechanics Approach. *Earth and planetary science letters*. 2012;**345**:72–80.
- [23] Zhang W Feizhou and Lu, Yan L, Ge Y. Research on Simulation Matching Algorithm of Underwater Passive Navigation System. *Journal of Wuhan University (Information Science Edition)*. 2003;**28**(2):153–157.
- [24] Yuan S, Sun F, Liu G, Chen J. Application of Gravity Graphic Matching Technology in Underwater Navigation. *Chinese Journal of Inertial Technology*. 2004;**12**(2):13–17.
- [25] Cheng L, Cai T, Xia B. A New Correlation Matching Algorithm in Gravity-Assisted Inertial Navigation System. *Journal of Instrumentation*. 2006;(z3):2235–2236.
- [26] Wang Z, Bian S. Gravity aided inertial navigation based on ICCP algorithm. *Journal of Surveying and Mapping*. 2008;**37**(2):147–151.
- [27] Zhang L, Yang H. Research on underwater terrain matching algorithm based on ICCP and TERCOM. *Journal of Projectiles and Guides*. 2008;**28**(3):230–232.

- [28] Zhang H. Research on Key Technologies of Underwater Gravity Field Assisted Navigation and Positioning; 2013.
- [29] Gong G. Autonomous underwater navigation method research; 2015.
- [30] Jolliffe IT. Principal Component Analysis. Springer-Verlag New York; 2002.
- [31] Baker W, Clem R. Terrain contour matching [TERCOM] primer. Technical Report ASP-TR-77-61 Aeronautical Systems Division, Wright-Patterson AFB. 1977;.
- [32] Golden JP. Terrain contour matching (TERCOM): a cruise missile guidance aid. In: Image processing for missile guidance. vol. 238. International Society for Optics and Photonics; 1980. p. 10–19.
- [33] Ma X, Yanli, Qiao Y. Matching region extraction method in Gravity Anomaly Aided Inertial Navigation. Journal of Surveying and Mapping Science and Technology. 2009;**26**(6):399–402.
- [34] Cheng L, ZHANG J Ya, Cai J Ti. Selection criterion for matching area in gravity aided navigation. Journal of Chinese Inertial Technology. 2007;**15**(5):559–563.
- [35] Ti-jing C, Xin-wei C. Selection criterion based on analytic hierarchy process for matching region in gravity aided INS. Journal of Chinese Inertial Technology. 2013;**21**(1):93–96.
- [36] Xia B, Cai J Ti. SPSS-based gravity matching region selection algorithm. Journal of Chinese Inertial Technology. 2010;**18**(1):81–84.
- [37] Liu F, Yao J. A local analysis method of marine gravity aided navigation area. In: Optoelectronics and Microelectronics (ICOM), 2013 International Conference on. IEEE; 2013. p. 5–9.
- [38] Shlens J. A tutorial on principal component analysis derivation. Discussion and Singular Value Decomposition. 2003;**25**.

- [39] Mahdi B, Taha H Hossein. A Mathematical Model Based on Principal Component Analysis for Optimization of Correlated Multiresponse Surfaces. *Journal of Quality*. 2012;**17**:223–239.
- [40] Danmei P, Cuijun D. Seletion of Suitable Matching Area in Gravit-Aided Inertial Navigation System. *Coordinates*. 2016;**12**:18–22.